**Proceedings of ASME Turbo Expo 2023
Turbomachinery Technical Conference and Exposition
GT2023
June 26-30, 2023, Boston, Massachusetts, USA**

**GT2023-103885**

# HIGH SPEED ROTARY ATOMIZER SUPPORTED ON POROUS TYPE GAS BEARINGS: CHALLENGES FACED, OPERABILITY DEMONSTRATION AND LOAD TESTING

**Vishal Wadhvani**
Dedert Corporation
Homewood, IL

**Claude Bazergui**
Dedert Corporation
Homewood, IL

**Paul Mehan**
New Way Air Bearings
Aston, PA

**Michael Smith**
New Way Air Bearings
Aston, PA

**Anthony Michael**
New Way Air Bearings
Aston, PA

## ABSTRACT

*A novel "patent-pending" high speed rotary atomizer supported on porous gas bearing technology was designed, fabricated and tested in response to challenges with an existing product on active magnetic bearing (AMB) technology and the desire to keep the design oil-free due to its inherent maintenance/ operation benefits. The lessons learnt on the magnetic bearing atomizer system especially in regards to the periodic rotor imbalances the atomizing process imposes on the system, scaling/ cost complexity of the design and the customer complaints/ feedback were at the heart of this new design endeavor on gas bearing technology. This paper describes all these issues in detail and the testing data on this new design is presented along with the challenges/ setbacks faced during the initial stages of prototype testing. Some of the failures experienced during the early stages of prototype testing will be described in detail (especially due to the temperature rise seen inside the machine at high operating speeds) and how some novel design improvements/ measures were undertaken to overcome them. Lastly, the benefits of this new design will be discussed in comparison to other bearing technologies and how they are being leveraged for use in multiple sizes so it can be a truly scalable platform.*

Keywords: Rotary Atomizer, Gas Bearing

## NOMENCLATURE

Nomenclature for the equations used in the paper is given below:

| | |
|---|---|
| $K_{tot}$ | Effective Stiffness (lbf-in) |
| $K_{o\text{-}ring}$ | O-ring Stiffness (lbf-in) |
| $K_{gas\ film}$ | Gas Film Stiffness (lbf-in) |
| $C_{tot}$ | Effective Damping (lbf-s/in) |
| $C_{o\text{-}ring}$ | O-ring Damping (lbf-s/in) |
| $C_{gas\ film}$ | Gas Film Damping (lbf-s/in) |
| $C_{xx,\ yy,\ tt}$ | Damping Coefficients (lbf-s/in) |
| $\mu$ | Dynamic Viscosity (lbf-s/in^2) |
| R | Radius of Bearing (in) |
| c | Gas Film Gap Height (in) |
| L | Length of Bearing (in) |
| D | Bearing Diameter (in) |
| K | Estimated Stiffness (lb-in) |
| D | Diameter of Bearing (in) |

## 1. INTRODUCTION

Spray drying is a method of producing dry powder from a slurry or liquid by rapidly drying the liquid with a hot gas stream. Spray drying is the preferred method of drying many thermally sensitive materials such as foods and pharmaceuticals. A consistent particle size distribution is a reason for spray drying some industrial products, such as catalysts and other chemicals. Typically, air is the heated drying medium; however, nitrogen may be used if the liquid being atomized is a flammable solvent (e.g., ethanol) or if the product is oxygen-sensitive. Generally, Spray dryers use an atomizer to disperse the liquid into a controlled-drop-size spray; common types of atomizers used include rotary disc and single-fluid pressure swirl nozzles. Depending on the process and/or product needs, drop sizes from 10 to 500 micrometers (0.00039 to 0.019 in.) may be achieved with the appropriate choices however common applications are often in the 100 to 200 micrometers (0.0039 to 0.0079 in.)

 

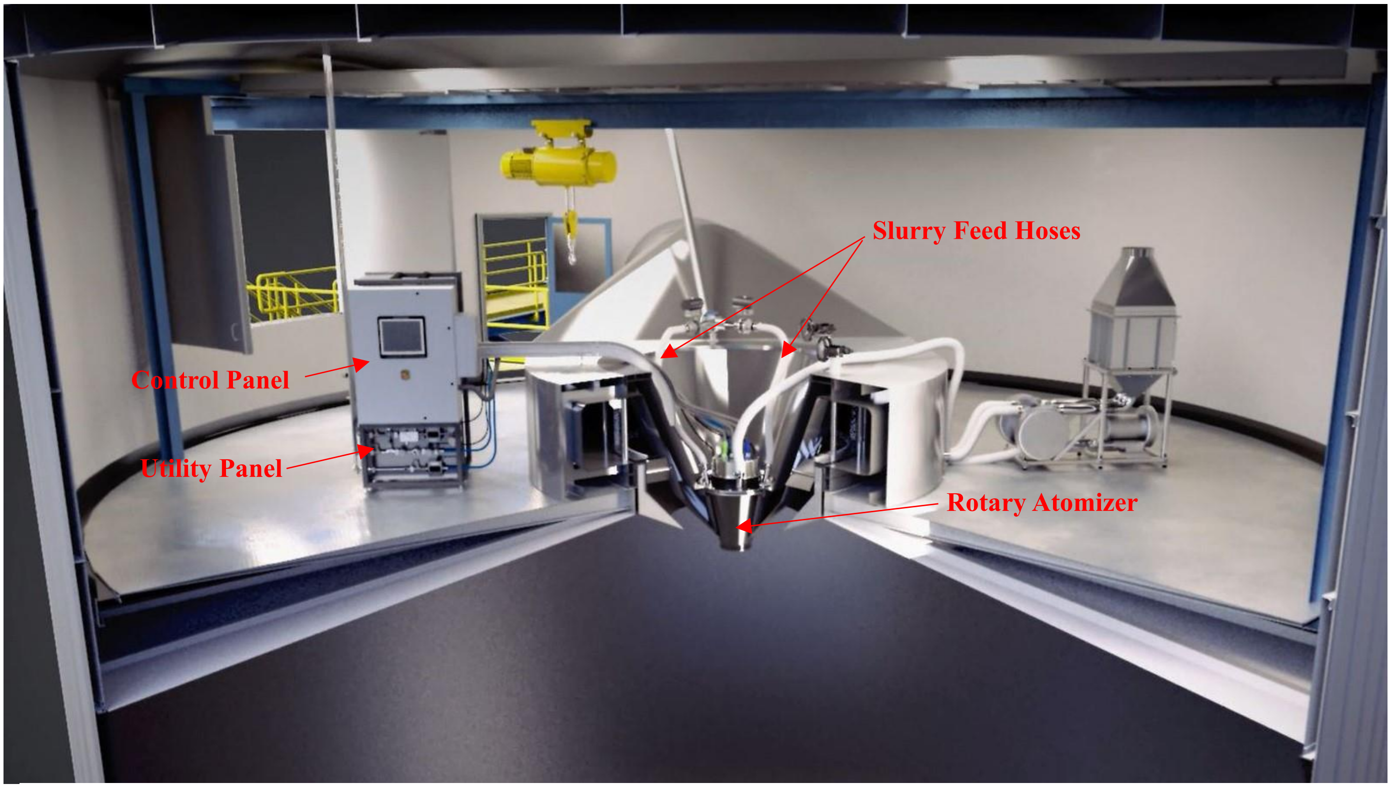


**FIGURE 1:** CUTAWAY RENDERING OF THE ATOMIZER SYSTEM

diameter range [1]. Figure 1 is a cutaway rendering of the atomizer installed in a spray dryer along with its control panel.

Conventional rotary atomizers have been used for many years and are still the norm in the industry – they comprise of an atomizer wheel drive shaft supported by oil lubricated spindle bearings or high-speed rolling element bearings and driven by a conventional induction motor through either a speed increasing gearbox or drive belt. These atomizers have several limitations including limited atomizer wheel surface speed, oil contamination in end-product, short bearing life and high maintenance lubrication systems or gear boxes. To address these limitations with existing products, a direct drive rotary atomizer with a permanent magnet motor supported on AMBs was developed and commercialized in 2012 however experience with multiple installations revealed the following:

1) Limited Bearing Load Capacity – In spite of the major improvements achieved in the operation of these machines as demonstrated in [1] and [2], there are still the daily intermittent contacts experienced during the operation of these machines. To add to these the rotor-drop events reported during some start-up/ shut-down sequences when there is residual slurry stuck on the disc, which would ultimately trip the main dryer system due to the interlocks, required a change of auxiliary/ backup bearing every ~1.5 years. All this points to limitation on the bearing load capacity given the exterior geometric constraints of the atomizer.
2) AMB Controller Parameters – Due to the client requirement of drying different products which required running the atomizer at different operation speeds for different batches, the AMB controller required different parameter files for continuous operation in different speed ranges e.g., for atomizer operation at low speeds of 5000 rpm a parameter file A was needed whereas when the operation speed was around 13000 rpm a parameter file B was needed which increased the software maintenance complexity.
3) AMB Controller Software Settings – The spray drying process necessitated the use of different atomizer wheel designs for different applications (e.g., Vaned wheel v/s an Insert Wheel v/s a Cup Wheel) which again required the correct parameter files to be installed for the peculiar disc design due to the difference in inertia and weight properties. At facilities using two different wheel designs, there was a manual requirement to ensure the correct parameter file is installed for the wheel in service.
4) Design Scaling/ Cost Complexity – Another limitation of the magnetic bearing technology was the fact that it did not scale down in size well enough for the low power (<150 kW/ 200 hp) applications without compromising the rotordynamic performance and many of the hard costs remained which included magnets, laminations, sensors, controller etc.
5) Indirect Customer Feedback – The plant machinery operators/ technicians in this industry have broad experience with traditional friction bearings due to their widespread use

in competitor machines and they could easily fix or develop a workaround in case of an emergency operation issue encountered during production however such is not the case with the magnetic bearing technology which required troubleshooting support directly from the OEM, due to the system complexity (sensor, actuator, controller etc.), and this added unwanted delays – some clients reportedly viewed this technology as a "black-box" where a lot checks/ things had to be in place for it to work normally. This technology required the end users to have trained personnel or supervisors who were intimate with the design on staff, and this wasn't always possible due to resource constraints especially since majority of the machinery on a spray dryer plant runs on traditional bearings.

Due to these limitations, the atomizer design experts at Dedert Corporation (Dedert)embarked to find other novel oil-free bearing technologies and decided to pursue the porous media gas bearings offered by New Way Air Bearings (New Way) after evaluating several other options keeping the above limitations close to heart. These gas bearings utilize a porous material as a means of feeding externally pressurized gas to the bearing shaft clearance region. This porosity of the material enables the pressurized gas to be distributed uniformly in the clearance region which results in a higher load capacity with very low flow consumption [3].

## 2. DESIGN OVERVIEW

A cross-section view of the 300 kW prototype rotary atomizer ABA-300, which was fabricated, is shown in Figure 2. The rotating shaft is supported in the radial direction by the top and bottom radial bearing assembly whereas a thrust bearing is employed for support in the axial direction. The slurry is fed via the two feed tubes which goes into the rotating wheel installed at the bottom of the shaft. The permanent magnet motor which enables the rotating motion is installed between the thrust bearing and the lower radial bearing. The exterior envelope of the 250 kW magnetic bearing atomizer MSM-250 was the design constraint since the project development goal was to directly compare the performance of gas bearings and magnetic bearings. Each radial bearing assembly comprises of 4 segmented porous gas bearing pads mounted in a cartridge and held in place via central bushings which also have an air supply opening as shown in Figure 3. There is a set of O-rings mounted between the pads and the cartridge along with a second set of O-rings mounted directly on the cartridge before it goes in the motor housing. This acts as a combination of springs in parallel and series which serve two purposes – reduce the stiffness of the gas bearings and damp out any rotor vibrations with adequate damping. The thrust bearing assembly comprises of two circular flat porous media pads which are mounted above and below the shaft collar with O-rings mounted behind each pad as shown in Figure 4.

The radial and thrust gas bearings ride at a fly height of approximately 400 to 900 microinches depending on the input air supply pressure and the load seen by the bearings. This air gap is very stiff (about 240,000 lbs./in to 405,000 lbs./in on the radial and 370,000 lbs./in to 2,900,000 lbs./in on the thrust measured at 100 psi supply pressure) [3] and is the mechanism that eliminates the friction between the bearing elements i.e. the rotating shaft and the bearing surface. This gap is then followed by two sets of clearances – one between the segmented pads and the cartridge which is of the order of 0.010in on the radius, other between the cartridge and the housing which is of the order of 0.009in on the radius. Together these two clearances allow for a total shaft movement of 0.038in on the diameter or peak to peak. Figure 5 shows the load-lift curves measured on the radial and

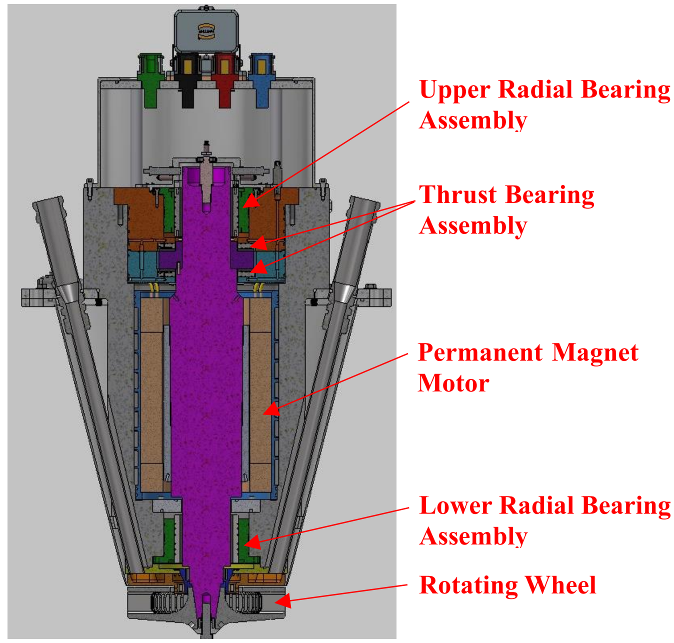


**FIGURE 2:** CROSS-SECTION VIEW OF THE ABA-300


**FIGURE 3:** RADIAL BEARING ASSEMBLY

**FIGURE 4:** THRUST BEARING ASSEMBLY PAD

thrust pads. These curves represent measurements on the individual pads and are much lower on the radial than the thrust primarily due to a smaller geometry (and hence area) besides other factors. However, the bearing stiffness of the complete gas bearing assemblies is intentionally and controllably reduced to meet the system requirements. The final effective radial stiffness is approximately 24,000 lbf./in at 15,000 rpm. This stiffness is determined via a combination of measured values, calculations, and extrapolations from known data sets.

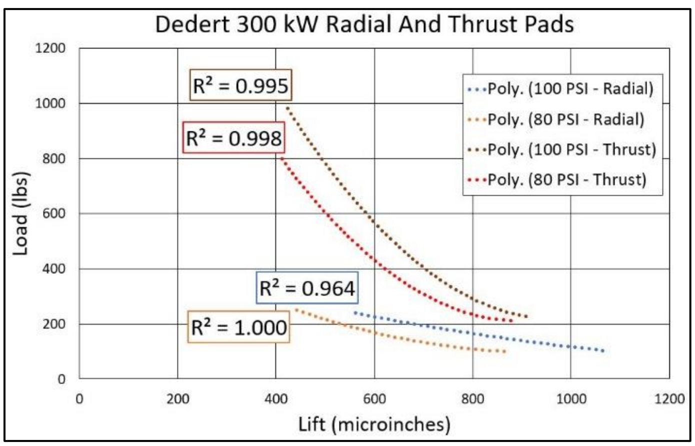


**FIGURE 5:** LOAD-LIFT CURVES OF THE GAS BEARINGS

## 2.1 Rotordynamic Analysis

Drawing upon the experiences from the magnetic bearing atomizer and to ensure a rigid shaft design, a conscious design effort was made to go with the biggest shaft diameter at the bearing locations ultimately iterating to a 100mm diameter. A rotordynamic analysis of the complete design was performed using Xlrotor software. The rotordynamics model of the shaft was built from a solid model. Figure 6 shows the Geo Plot of the completed model. Axial tension was added to each station which accounted for the effect of gravity on the response of the vertically mounted shaft. Added masses were used to account for the mass and the polar and transverse moments of inertia for the motor rotor and disk. The primary rotordynamic coefficients are stiffness and damping. The stiffness and damping coefficients comprise two components: the gas film and the compliant bearing mount. In this design, the gas used is air, and

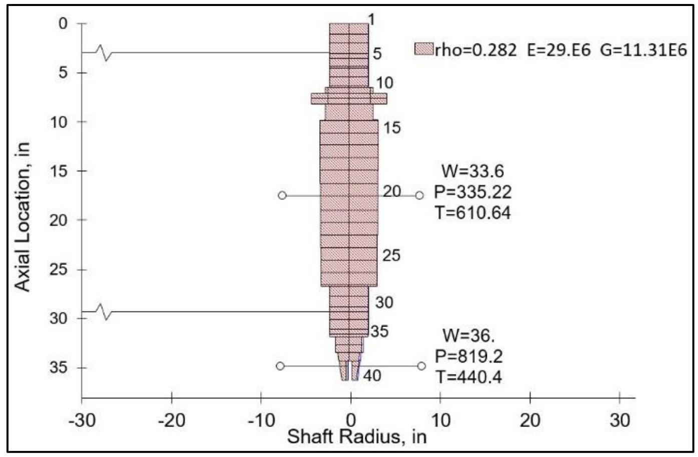


**FIGURE 6**: GEO PLOT FOR 300 kW PROTOTYPE ATOMIZER

the bearings are compliantly mounted on O-rings. The two components act similarly to a spring-mass-damper system in series. The effective stiffness (K) and damping (C) of the bearings can be calculated in accordance with the following equations, respectively.

$$\frac{1}{Ktot} = \frac{1}{Ko-ring} + \frac{1}{Kgas\,film}$$

$$\frac{1}{Ctot} = \frac{1}{Co-ring} + \frac{1}{Cgas\,film}$$

The gas film damping can be calculated using the following equation which is dependent on the dynamic viscosity, the height of the bearing gap and the bearing geometry [5].

$$Cxx = Cyy = Ctt = 12\pi \frac{\mu R^3 L}{c^3}\left[1 - \frac{\tanh\left(\frac{L}{D}\right)}{\left(\frac{L}{D}\right)}\right]$$

The gas film stiffness for the prototype was calculated based on empirical data gathered by New Way from similar products of varying sizes (i.e. x1, x2, y1 and y2 are known data). Linear interpolation as seen below is used for similar products of varying sizes.

$$K = x_1 + (x_2 - x_1)\left(\frac{D - y_1}{y_2 - y_1}\right)$$

The o-ring stiffness and damping are both speed dependent. Significant empirical data exists that is used to estimate the stiffness and damping of the o-rings. The empirical data was measured with the following independent variables: material, squeeze, cross-sectional diameter, stretch, temperature, groove width, amplitude, and frequency. Interpolation is used to calculate stiffness and damping for specific configurations that do not match the exact test conditions. The analysis was performed using data for two pairs (four per bearing) of

VITON™ 70 durometer O-rings behind the tilt pads and two pairs (four per bearing) behind the cartridge. As the cartridge is allowed to move in this design, these o-rings were included in the stiffness and damping calculations.

Assumptions made in this analysis include symmetrical stiffness and damping $K_{xx} = K_{yy}$ and $C_{xx} = C_{yy}$. Cross coupling terms for tilt pad gas bearings are usually neglected at slow speeds and while increasing with speed are considered of small magnitude, therefore we assumed $K_{xy} = K_{yx} = 0$ and $C_{xy} = C_{yx} = 0$. These assumptions were felt to be justified by the vertical arrangement of the shaft.

Figure 7 shows the undamped critical speed map which shows the first bending mode appears to be around 40,000 RPM. When damping is accounted for, the only natural frequency that crosses the synchronous line is a backward whirl mode shape at 17,500 RPM as shown in Figure 8. Backward modes are typically disregarded and not excitable. All excitable natural frequencies are safely outside the operating range.

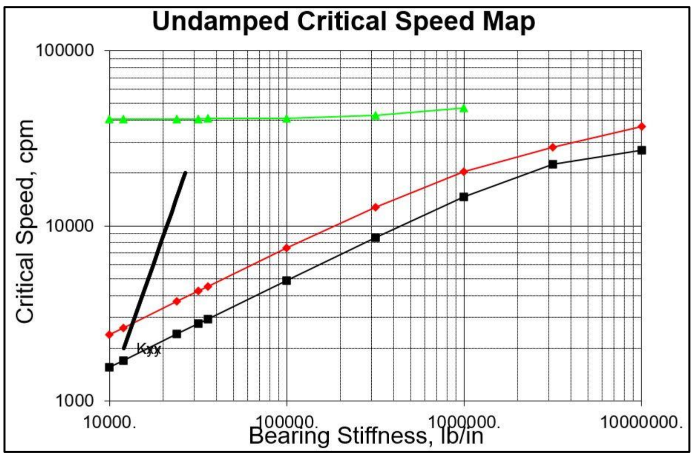


**FIGURE 7:** UNDAMPED CRITICAL SPEED MAP FOR 300 kW PROTOTYPE ATOMIZER

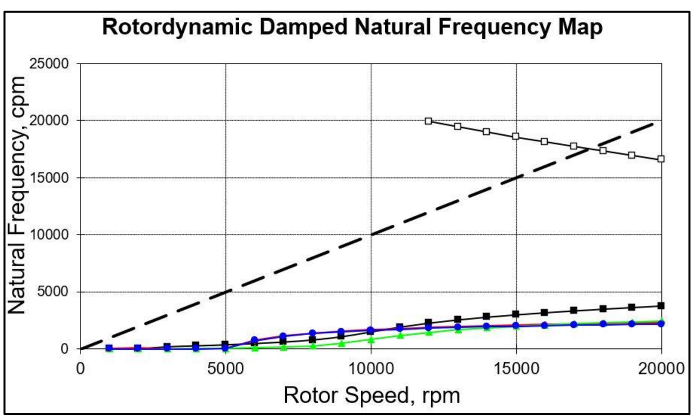


**FIGURE 8:** DAMPED NATURAL FREQUENCY MAP FOR 300 kW PROTOTYPE ATOMIZER

Response calculations using assumed levels of unbalance more than typical permissible unbalance including one at 50% greater than known field unbalances were run. Figure 9 shows a typical response plot. All amplification factors seen indicated that the peak responses were "well-damped". All peak-to-peak shaft displacements were acceptable in the speed range. These conclusions were verified by subsequent testing. An L/D ratio of 1 was maintained on the radial gas bearing pad designs due to the prior experience at New Way. Table 1 summarizes the bearing load capacities, computed assuming a 100-psi supply input pressure, which were used for this prototype.

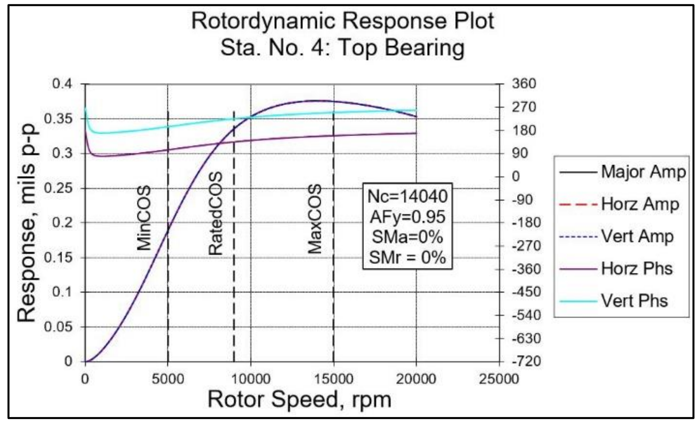


**FIGURE 9**: RESPONSE PLOT FOR 300 kW PROTOTYPE ATOMIZER

**TABLE 1**: CALCULATED LOAD CAPACITIES

| | **Radial** | **Axial** |
|---|---|---|
| **Bearing Load Capacity** | 645 lbf | 1400 lbf |

## 2.2 Risk Mitigation

Early in the design phase, it was decided to evaluate the performance of the gas bearings under conditions of impulse loading, which are encountered in actual site conditions as concluded in [1] and [2], for risk mitigation purposes and implement any tweaks to the design. From [2], it was known that the minimum imbalance seen by the disc was 70 gm-in and that resulted in a backup bearing load of about 2250 lbf at the operating speed of 13000 rpm. This information was used as the basis for designing a rig, shown in Figure 10, to test the bearings under these impulse loading conditions. The shaft was spun upto 15000 rpm and the impact hammer was released from a predetermined height to create an impact force of 6000 lbs. (about 2.5 times higher than seen on the field with the MSM-250) – the bearings withstood the impact, without any issues reported, with a maximum displacement recorded around 0.030in and adequate damping achieved on the resulting rotor vibration as shown in Figure 11.

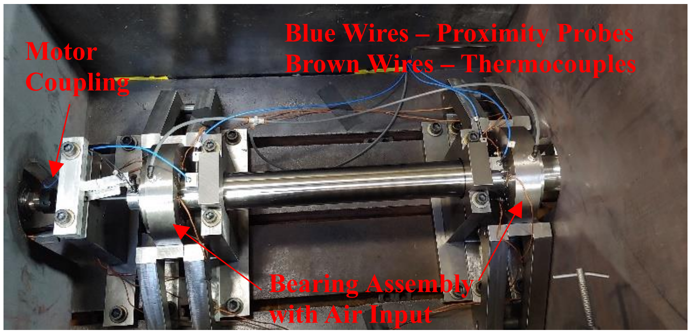


**FIGURE 10a:** ROTATING SHAFT SUPPORTED BY TWO BEARINGS IS MOUNTED IN A STEEL ENCLOSURE

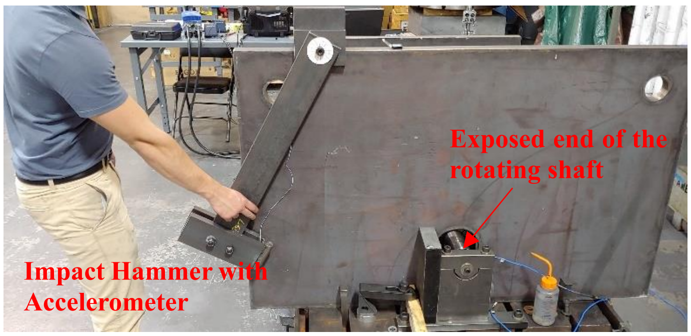


**FIGURE 10b:** IMPACT HAMMER WITH ACCELEROMETER IS RELEASED FROM A PREDETERMINED HEIGHT

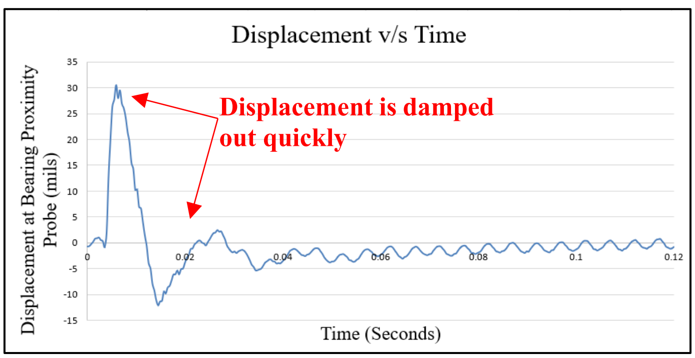


**FIGURE 11:** DISPLACEMENT V/S TIME AT BEARING PROXIMITY PROBE

## 3. CHALLENGES FACED DURING INITIAL TESTING

An initial limited round of testing (limited on motor speed & power) was conducted on the prototype unit in the month of November 2019, and this proved successful in all aspects since all the motor/ bearing parameters showed acceptable performance. The limitation was mostly on the variable frequency drive (VFD) aspect since the full horsepower drive wasn't readily available due to resource constraints. Soon after the successful limited test run, some design enhancements were made to improve the prototype design while waiting for the new drive. Delays due to COVID-19 pushed the full power testing with the new VFD until April 2021 and that is when multiple issues were observed on the system.

During two such instances, just with only about 1 hour of runtime on the bearings at increasing speeds all the way to the full speed of 15000 rpm caused the atomizer to crash on the bearings i.e., experience supply air pressure loss and ultimately cause rubbing of the rotating shaft with the gas bearing pads. A further investigation into the root cause revealed that the temperature rise was mostly localized near the lower thrust bearing, and it was this bearing which was failing due to high temperature. Figure 12 shows an image of the bottom surface of the collar where temperatures reportedly reached around 350 °C. A deeper dive into all the design changes made after the successful 2019 run and after sifting through all the runtime data, the following changes were made to address the relevant issues which were discovered.


**FIGURE 12:** THRUST COLLAR WEAR WITH TEMPERATURE DISCOLORATION

- Temperature Measurement of the Thrust Pads/ Shaft Collar

Due to the novelty of the design, the local heat accumulation/ generation and thus the high temperature rise seen in the lower thrust bearing section wasn't envisioned which led the development team to operate blind or have no temperature feedback from this section during the initial test runs. However, after the back-to-back crashes on the atomizer and reviewing the points of failure, a design change was made to employ non-contact infrared temperature sensor for detecting the temperature rise in the region and start gauging the sensitivity of any or all operating condition changes on this parameter.

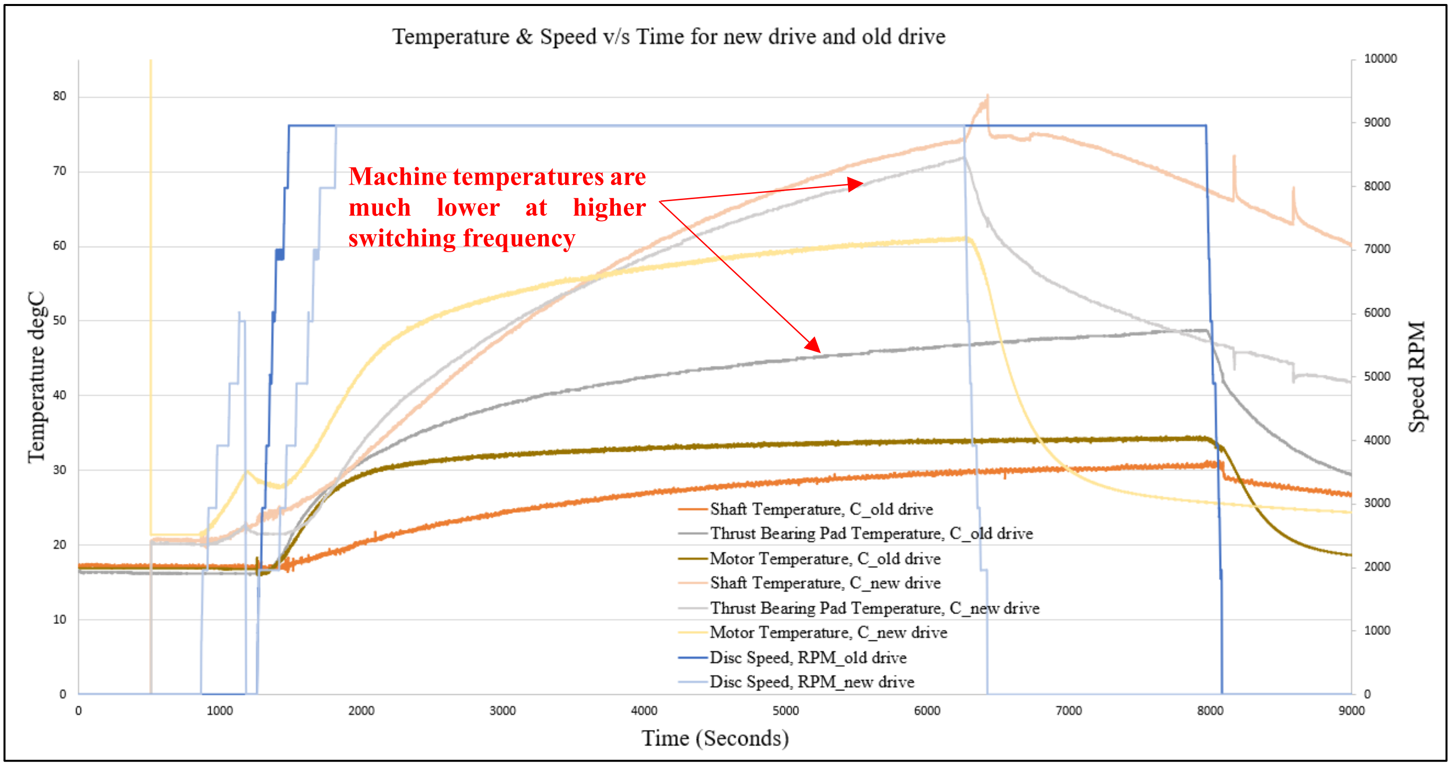


**FIGURE 13**: MACHINE PARAMETERS TEMPERATURE TREND WITH OLD AND NEW DRIVE

- VFD Switching Frequency/ Sine Filter Design

In ensuring the new full horsepower drive complies with the internal system level design preferences, an important aspect of the drive switching frequency/ sine filter design was overlooked and was discovered only when full power/ maximum speed testing began with the new drive. The original VFD had an 8 kHz switching frequency with 33 µF capacitance per phase on the sine filter whereas the new VFD had only a 4 kHz switching frequency with 144 µF capacitance per phase on the sine filter – the motor vendor had recommended a 8 kHz switching frequency with appropriate capacitance on the sine filter to operate the motor windings at higher efficiencies (or lower losses thus lower temperatures). While the new combination of lower switching frequency and higher capacitance was still acceptable for the motor performance, the resulting extra heat via losses from the windings was causing the temperature rise on the thrust pads due to the very small air gap it operates with. To minimize

the shaft collar/ thrust pad temperature rise and not do a complete overhaul of the machine layout, another new full horsepower drive with the higher switching frequency of 8 kHz and lower sine filter capacitance of 33 µF per phase was employed for all further testing which improved the temperature profile of all the parameters. Figure 13 shows the temperature of the machine parameters with the two drives while running at a nominal speed of 9000 rpm.

- Thrust Pad Preload and Adequate Cooling

One of the other main reasons discovered for the temperature rise seen in the thrust bearing section was the heat generation due to shear in the lower thrust bearing air gap. This shear heating increases with load, since increasing the load reduces the bearing gap. The shear heating was found to be directly influenced by the preload on the thrust bearings, the initial design of which was set to have a value of 725 lbs. A series of design iterations were conducted by reducing the collar thickness and the O-ring durometer to reduce this value to roughly 385 lbs. This lower preload resulted in reduced shearing in the air gap which was found to have the lowest temperature rise on the bottom thrust bearing pad along with acceptable behavior of the vibration experienced by the machine during operation upto full speed. It might be argued to not have this preload at all for best thermal performance, but this preload is an actual designed load which is a characteristic of this gas bearing design. In addition to reducing the thrust bearing preload, a stream of motor cooling air was also directed towards this region and that helped lower the temperature equilibrium as well.

## 4. QUALIFICATION TESTING AND DISCUSSION

Once these initial challenges/ issues were addressed, an internal test plan was developed to define successful qualification of the machine before commercialization and below three test conditions were developed:

a) 8-hour runtime on the machine at maximum speed and unloaded condition
b) 48-hour runtime on the machine at maximum speed and maximum load condition achievable on the test bed
c) Unbalance testing of the machine by running it to full speed with a 105 gm-in disk imbalance (50% higher

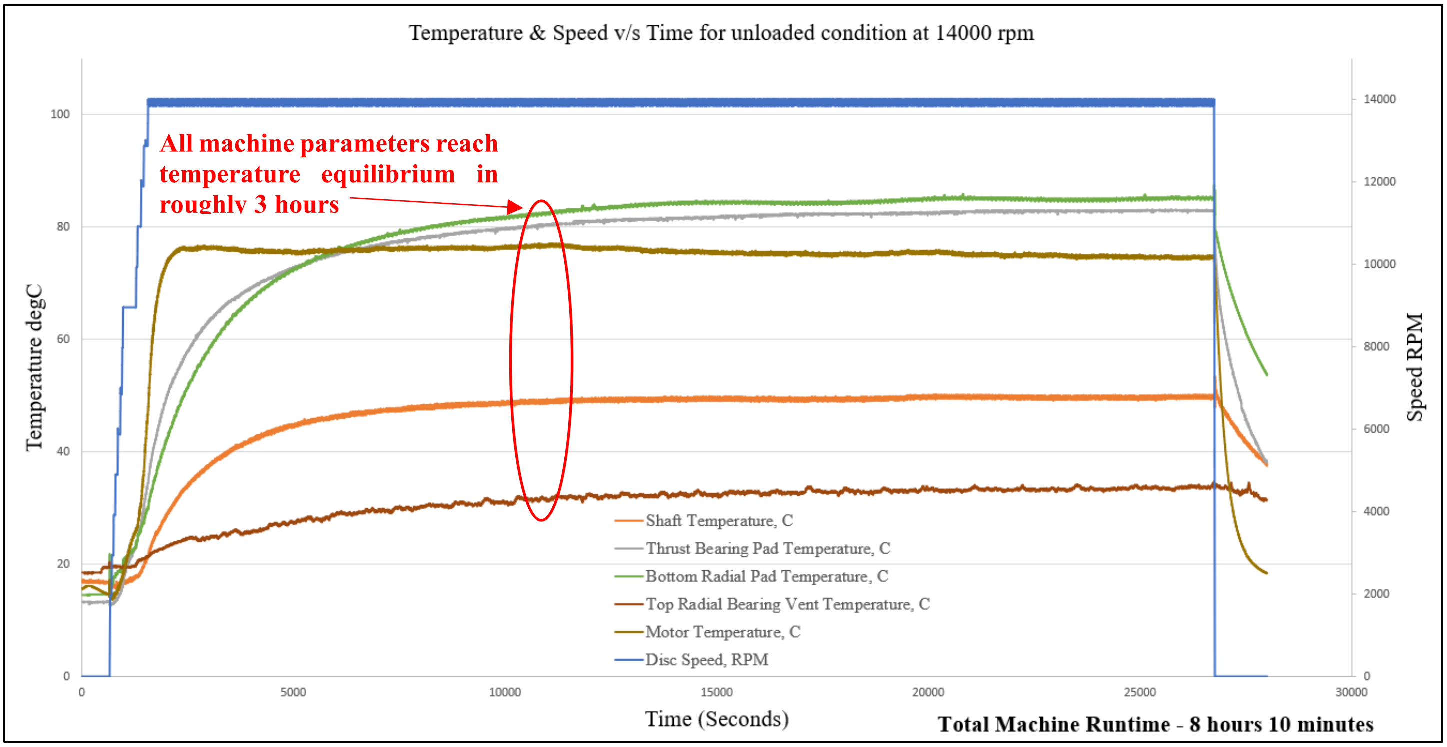


**FIGURE 14**: MACHINE PARAMETERS TEMPERATURE TREND FOR TEST CONDITION A

imbalance than seen on the field) and run at this state for 20 minutes

All the above three test conditions were designed to capture adequate runtime on the system after it had achieved equilibrium state for all machine temperature parameters and bearing vibration. The prototype successfully passed the test conditions a) and c) however the test bed setup was seen struggling during extended duration run under test condition b) at only 4 hours of runtime. The modifications required on the test bed for test condition b) would have required a significant investment along with a considerable delay to the project while only providing a psychological comfort since the three test conditions were internally developed. To overcome this, it was decided to conduct 4 hours of runtime daily on the system at maximum load for a week and ensure repeatability of the data on all the machine parameters which again the prototype successfully passed.

Figure 14 and 15 show runtime temperature trends of the machine while running under test condition a) and modified test condition b). As seen from Figure 15, all machine parameters reported elevated temperature levels under loaded condition and the system fails to achieve temperature equilibrium due to the test bed setup. The system now awaits installation and 24x7 testing at an actual customer site to confirm the viability of this new technology while offering a very promising solution to the problems that the atomizer design experts at Dedert originally intended to solve.

This gas bearing technology promises to offer the same oil-free, reliability and maintenance benefits as the AMB technology but at a more affordable/ competitive price and without any software complexities i.e., maintenance personnel and shop floor technicians can much better relate to the technology similar to the conventional bearings. The load carrying capacity of these bearings is also much higher in the same geometric footprint [4]. All these benefits add up to make it an attractive option for the rotary atomizer application. When comparing these bearings to the conventional friction bearings, the only drawback is that these gas bearings are expensive, but the overall technology is still very attractive since it offers the superior benefits of an AMB technology [4].

## 5. CONCLUSION

A novel design of a rotary atomizer on porous gas bearing technology is presented in response to challenges presented by the AMB technology on a similar application. This new design offers similar superior benefits of an AMB technology like oil-free design, high reliability, and low maintenance but at a more affordable price and no control software complexities which makes it an attractive option for this application. The challenges faced during the initial testing are presented and the relevant measures taken to address them are discussed.

The prototype has been fully tested to the maximum extent possible in the testbed setup and now awaits testing at an actual client site under real world conditions. Due to the promising test results seen on this prototype, production work on a 300 kW, a 100 kW and a 25 kW rotary atomizer using this porous gas bearing technology is underway at full steam and the goal is to commercialize these product lines within this year.

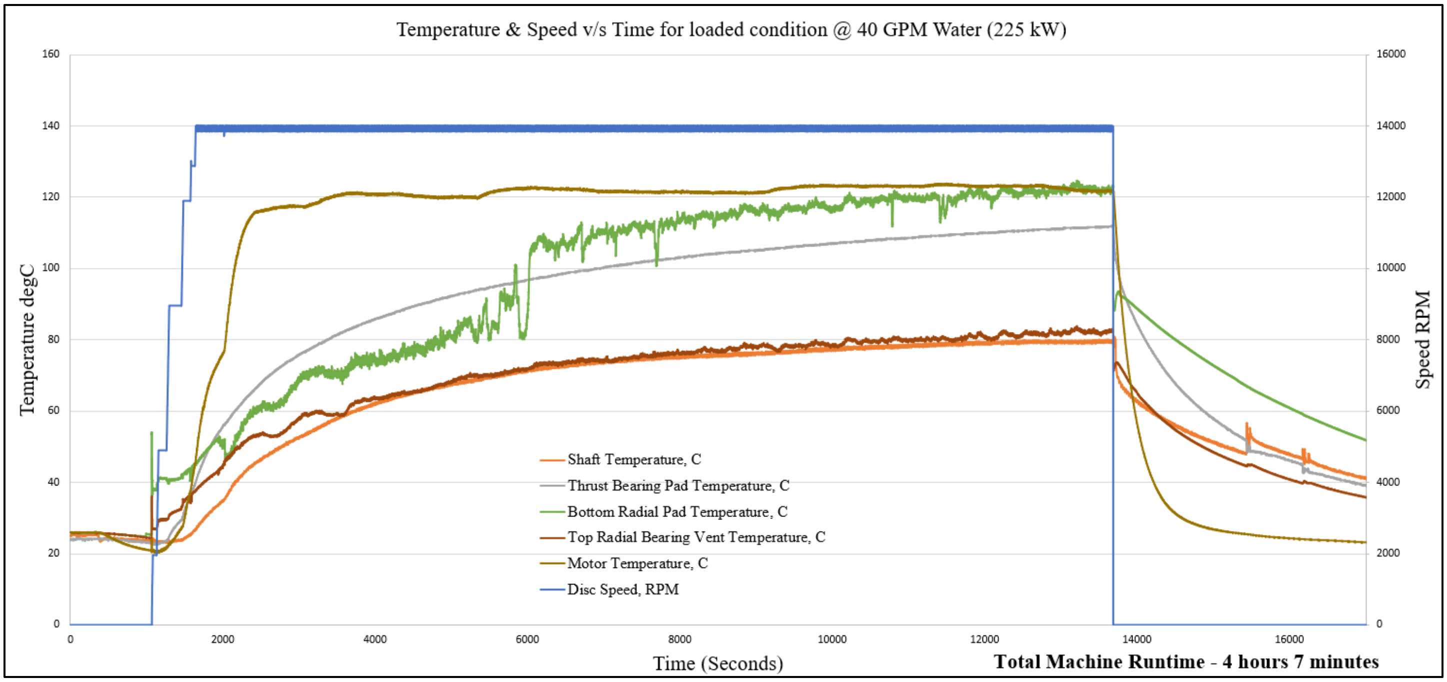


**FIGURE 15**: MACHINE PARAMETERS TEMPERATURE TREND FOR MODIFIED TEST CONDITION B

## ACKNOWLEDGEMENTS


The authors of this paper would like to thank the executive management teams at Dedert Corporation and New Way Air Bearings for their continued financial support and patience with this program despite the numerous setbacks/ delays faced during its development.


## REFERENCES


[1] Khatri, R., Hawkins, L., Bazergui, C., "Demonstrated operability and reliability improvements for a prototype high-speed rotary-disc atomizer supported on active magnetic bearings", ASME Turbo Expo 2015, Paper GT2015-43803, June 15-19, Montreal, CA

[2] Hawkins, L., Wang, Z., Wadhvani, V., "Transient simulation of magnetic bearing and backup bearing interaction in a high-speed rotary atomizer subjected to impulsive loads", International Symposium on Magnetic Bearings 2016, Paper ISMB15 – 10051, August 3-6, Kitakyushu, JP

[3] San Andres, L., Cable, T., Zheng, Y., Santiago, O., Devitt, D., "Assessment of porous type gas bearings: Measurements of Bearing Performance and Rotor Vibrations", ASME Turbo Expo 2016, Paper GT2016-57876, June 13-17, Seoul, ROK

[4] https://bentlybearings.com/technical-information/

[5] San Andres, L., "Squeeze Film Dampers – Operation, Models and Issues of Interest", Texas A&M Machinery Vibrations and Rotordynamics Short Course, January 9-13, 2017, Houston, TX, p. 23